

Computational Fluid Dynamics and Thermal Analysis of an Unloaded Lumber-drying Kiln

Yasin Furkan GÖRGÜLÜ , Murat AYDIN* 

Isparta University of Applied Sciences, Keciborlu Vocational School, Department of Machine, Isparta, TÜRKİYE

*Corresponding Author: murataydin@isparta.edu.tr

Received Date: 18.05.2022

Accepted Date: 14.02.2023

Abstract

Aim of study: Drying in kilns becomes one of the most significant procedures for the optimal use of wood products since the dimensions alter with changes in relative humidity. Computational fluid dynamics analysis of an unloaded lumber-drying kiln and positioning of the timber to be dried were aimed.

Material and methods: The heat and flow analysis of the lumber-drying kiln was analyzed using ANSYS software. Concrete and aluminum were chosen as the floor and wall materials, respectively. The wall thickness was taken as 1 meter. Gravity forces were also taken into account in the study, the number of elements of the created mesh is 87057 and the number of nodes is 17730.

Main results: The flow characteristics and temperature analyses formed in the study shed light on the lumber-drying kilns planned to be built. Preliminary information is provided about the positioning of the lumbers to be dried according to flow paths and temperature distributions.

Highlights: Flow analyzes of the unloaded lumber-drying kiln were undertaken and streamlines were shown. The thermal analysis of the hot air directed from the fans together with the concrete floor of the drying kiln and the walls made of aluminum panels was made.

Keywords: ANSYS, Computational Fluid Dynamics, Heat transfer, Lumber drying, Streamlines

Boş Kereste Kurutma Fırının Hesaplamalı Akışkanlar Dinamiği ve Isıl Analizi

Öz

Çalışmanın amacı: Ahşap ürünlerin boyutları bağlı nemdeki değişikliklerle değiştiğinden, fırınlarda kurutma, ahşap ürünlerin optimum kullanımı için en önemli prosedürlerden biri haline gelmektedir. Yüksüz bir kereste kurutma fırınının hesaplamalı akışkanlar dinamiği analizi ve kurutulacak kerestenin konumlandırılması amaçlanmıştır.

Materyal ve yöntem: Kereste kurutma fırınının ısı ve akış analizi ANSYS yazılımı kullanılarak yapılmıştır. Zemin ve duvar malzemesi olarak sırasıyla beton ve alüminyum seçilmiştir. Duvar kalınlığı 1 metre olarak alınmıştır. Çalışmada yerçekimi kuvvetleri de dikkate alınmış, oluşturulan ağırlık eleman sayısı 87057 ve düğüm sayısı 17730'dur.

Temel sonuçlar: Çalışmada oluşturulan akış özellikleri ve sıcaklık analizleri, yapılması planlanan kereste kurutma fırınlarına ışık tutmuştur. Kurutulacak kerestelerin akış yolları ve sıcaklık dağılımlarına göre konumlandırılması hakkında ön bilgiler verilmektedir.

Araştırma vurguları: Yükleme yapılmamış kereste kurutma fırınının akış analizleri yapılmış ve akım çizgileri gösterilmiştir. Kurutma fırınının beton zemini ve alüminyum panellerden oluşan duvarları ile birlikte fanlardan yönlendirilen sıcak havanın termal analizi yapılmıştır.

Anahtar Kelimeler: ANSYS, Hesaplamalı Akışkanlar Dinamiği, Isı transferi, Kereste Kurutma, Akım çizgileri

Introduction

Lumber must be dried prior to processing hygroscopic wood material to prevent specific flaws or failures. For this purpose, natural and engineered drying processes are applicable. When fresh timber is exposed to ambient air, it naturally dries to an equilibrium moisture

content (EMC) which varies according to location and season. However, it should be dried to the target moisture content (MC) of the utilization site. Therefore, drying is the primer and crucial process for the production and utilization of wood or wood-based products. But, improper drying of wood



causes drying faults such as bow, cup, bend, twist, and checks. The rupture of wood tissue, warp, uneven MC, and discoloration are classification types for defects that occur during and after drying (Ward, 1991).

Air (natural) and kiln (artificial or engineered to increase drying rate) drying are two main methods for drying wood and some recent studies are (Budakçi et al., 2018; Guler & Dilek, 2020; Lee et al., 2022; Tarmian et al., 2022) for radio or high-frequency vacuum drying, (Dulău & Madaras, 2019) for kiln monitoring and control system development, (Janjai et al., 2010) for development of solar timber drying system, (Korkmaz et al., 2020) for energy efficiency of drying using solar energy, (Görgün & Ünsal, 2020) for continuous lumber drying kilns, (Korkut et al., 2018; Ünsal et al., 2020) for drying schedules optimization or comparison, (Aydın & Colakoglu, 2008) for steaming and high-temperature drying, (Özşahin et al., 2019) for veneer drying temperature optimization, and (Ciritcioğlu et al., 2022) for check detecting while drying. Conventional, dehumidification, and vacuum are the types of kilns and have different advantages and disadvantages such as capacity, cost (installation, operation, and maintenance), ease of use, etc. According to Hızıroğlu (2017), dehumidification kilns are the most commonly operated kilns because conventional kilns (Figure 1) require a high amount of energy, and vacuum kilns have limited capacity. The cost of energy increases

day by day and the efficiency of the used energy should be evaluated for competition in wood drying. The aim of this study was the figure out the efficiency of a conventional kiln with a modified layout of basic configuration (Figures 1 and 2) by figuring out the streamline and temperature contours. Computational Fluid Dynamics (CFD) is a powerful tool used to analyze the flow of air within a wood-drying kiln. CFD is used to simulate the airflow patterns inside the kiln and to study the impact of different variables, such as temperature and humidity, on the drying process. CFD can also be used to optimize the design of a wood-drying kiln, to ensure that the drying is done efficiently with minimum energy expenditure. Additionally, CFD can be used to analyze the emissions of a wood-drying kiln and to evaluate the effectiveness of different technologies to minimize these emissions (Bian, 2001; Hughes & Oates, 2011; Vaz et al., 2013). Ghiaus et al., (2010) performed a CFD study on drying wooden pallets. Fluent was used in the analysis and the k-epsilon turbulence model was chosen. As a result of the study, velocity vectors and flow paths were examined. In wood drying CFD studies, different air inlet and outlet duct directors were designed and its suitability was examined (Hui-hui et al., 2015). Smit et al. (2007) analyzed the modeling of the flow passing through the wood piles, defining the wood pile as a porous media.

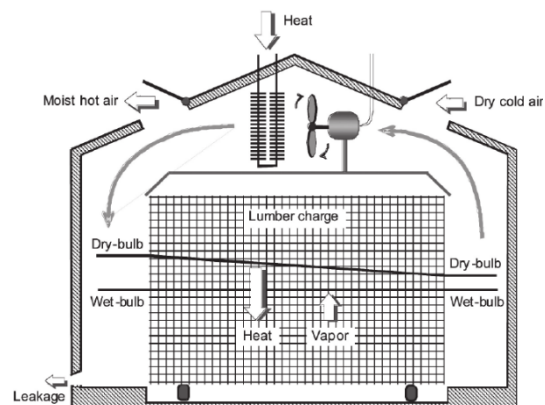


Figure 1. Left; A conventional lumber-drying kiln (Tuscarora Wood Midwest, 2021), and Right; Basic configuration for kiln drying of lumber (Elustondo & Oliveira, 2009)

Materials and Methods

Lumber-drying Kiln Design

The outer dimensions of the drying kiln are 8 x 13 x 4 meters in width, length, and height, respectively. In conventional lumber-drying kilns, fans are generally positioned parallel to the ground in terms of flow direction (see Figure 1.). In the drying kiln designed in the study, the fans are positioned perpendicular to the ground. The fans planned to be used in the designed kiln have a diameter of 1.5 meters and are designed as 8 equidistantly. Ten chimneys have been placed in order to evacuate the air easily. The kiln design, inlets, and outlets are shown in Figure 2. The parts shown in red represent the fans and therefore the air inlets. The parts shown in blue show the air discharge channels and the parts shown in grey illustrate the aluminum kiln walls. Hot air enters through the inlets and completes its cycle inside the kiln and exits through the outlets. The fans are 1.5 meters in diameter and the chimneys are 1 x 1 meter. In the real-life kiln application, the kiln interior is set to be 60°C, so the air inlets in the simulation are also determined to be 60°C. In wood production, a large amount of sawdust and parts that cannot be used for drying come out. In order to evaluate them, these sawdust and wood residues will be used in the heating system and it is thought to be supported by solar energy systems. Aluminum is used as the wall panel material, as in most real-life applications. The base material is defined as concrete. The thickness of the concrete wall is defined as 1m.

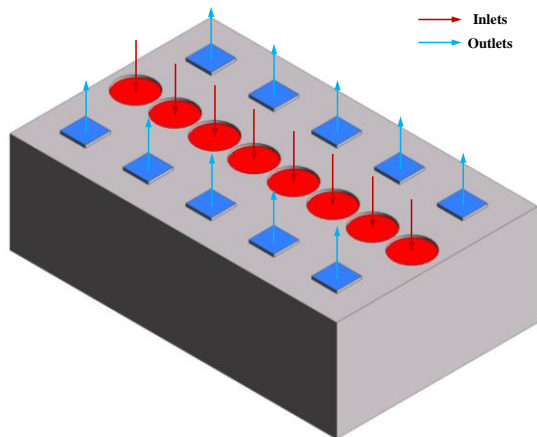


Figure 2. The three-dimensional kiln design

The kiln is designed as empty, that is, unloaded, and it is planned to place the lumber to be dried according to the flow and temperature distribution.

Computational Fluid Dynamics (CFD)

CFD is a method for solving equations that control fluid flow within a particular flow shape. The creation of a CFD model necessitates a precise characterization of parameters, a decision on numerical methods and mathematical equations, initial and boundary conditions, and appropriate empirical correlations that describe the process (Jamaledine & Ray, 2010). The Navier-Stokes transport equations may be used to explain the flow of any fluid. Standard textbooks and published articles include detailed explanations of CFD and analyses of pre-processing, processing, and post-processing (Fletcher, 1998; Kuriakose & Anandharamakrishnan, 2010; Marshall & Bakker, 2009; Sun, 2007; Versteeg & Malalasekera, 2007; Xia & Sun, 2002). Mass, momentum, and energy conservation equations are the primary governing equations in fluid mechanics and heat transfer. The following equations show how intended flow characteristics vary in response to external forces (Norton & Sun, 2006):

The law of conservation of mass states that the mass flowing into a fluid system must equal the mass flowing out. Mass is neither generated nor destroyed but rather transported from one spot to another, as stated in the Equation 1 (Bernard & Wallace, 2002; Erriguible et al., 2005; Erriguible et al., 2006; Norton et al., 2007). Concentration gradients are the driving factor behind this movement. The one-dimensional expansion of the continuity equation on the x-axis is given below:

$$\frac{\partial \rho}{\partial t} + \rho \nabla \cdot \bar{u} = 0 \quad (1)$$

The total of external forces acting on a fluid particle equals its rate of change in linear momentum, according to Newton's second law of motion. For fluid motion in the x-direction, the Euler equation (Eq. 2) is:

$$\frac{\partial(\rho u_i)}{\partial t} + \nabla \cdot (\rho u_i \bar{u}) = -\nabla p + \rho g \quad (2)$$

The heat addition and work done on a fluid particle equal the rate of change of energy of the particle., according to the first rule of thermodynamics. In the x-direction, the energy balance equation is (Eq. 3):

$$\rho C_p \frac{\partial T_f}{\partial t} + \rho C_p u_i \nabla T_f = -\lambda \nabla^2 T_f + S_T \quad (3)$$

CFD simulations mainly consist of three parts. These are the creating the geometry, meshing, and computational domain (defining boundary conditions, solving methods, flow parameters, and so on.). The geometry's design was created using Ansys' DesignModeler and SpaceClaim plugins. In the kiln design, 8 air inlets, in other words, fans, and 10 air evacuation channels, namely chimneys, were determined. There are 8 inlets and 10 outlets in total in the geometry.

The number of elements of the created mesh is 87057 and the number of nodes is 17730. The mesh structure created is shown in

Figure 3. The maximum skewness value recommended by Ansys is to be less than 0.95 and the minimum orthogonal quality value to be greater than 0.1. The maximum skewness of the mesh used in the study is 0.84 and this value is considered "Acceptable" by Ansys. The minimum orthogonal quality value is 0.15, this value is also considered "Acceptable". The quality scale of these two parameters is given in Tables 1 and 2 (Ansys Inc., 2011, 2015; Görgülü et al., 2021).

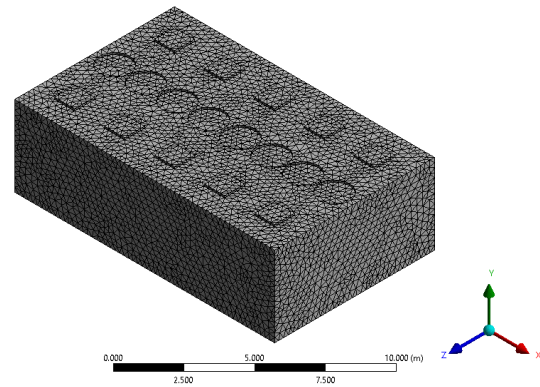


Figure 3. The three-dimensional mesh structure of the kiln design

Table 1. The skewness mesh quality metrics spectrum

Excellent	Very good	Good	Acceptable	Bad	Unacceptable
0.00-0.25	0.25-0.50	0.50-0.80	0.80-0.94	0.95-0.97	0.98-1.00

Table 2. The orthogonal quality mesh metrics spectrum

Unacceptable	Bad	Acceptable	Good	Very good	Excellent
0.000-0.001	0.001-0.100	0.100-0.200	0.200-0.690	0.700-0.950	0.950-1.000

The drying temperature was observed as a range of 35-60°C in the companies that visited in the field. Therefore, in the simulation, the inlet temperature was entered as 60°C (333 K). Similar to the applications, the flow velocity is taken as 5 m/s. Gravitational forces were also taken into account in the analysis and were taken as 9.81 m/s² in the -y-direction. One of the most well-known and widely used two-equations Eddy Viscosity model is the k-ε model (Jones & Launder, 1972; Launder & Sharma, 1974; Wilcox, 2006). For free shear layer flows with minor pressure gradients, this model has shown to be quite accurate. The model agrees well with experimental data for zero and modest mean pressure gradients for wall-constrained flows, but it is less accurate for high unfavorable

pressure gradients. The model's predictions are unaffected by turbulence in freestream. The model necessitates the use of precise grid spacing near solid walls, as well as explicit wall-damping mechanisms (Bardina et al., 1997; Rumsey, 2021). Therefore; in the simulation, realizable k-ε was preferred as the turbulence model. The Reynolds stresses are characterized as follows in terms of Eddy Viscosity (Eq. 4) (Bardina et al., 1997):

$$\tau_{ij} = 2\mu_t(S_{ij} - S_{nn}\delta_{ij}/3) - 2\rho k\delta_{ij}/3 \quad (4)$$

As a function of turbulent kinetic energy, k, and turbulent dissipation rate, ε, the eddy viscosity is defined as (Eq. 5):

$$\mu_t = c_\mu f_\mu \rho k^2 / \varepsilon \quad (5)$$

The following are the turbulence transport equations for the k- ε Launder-Sharma model (Eq. 6-7):

Turbulence energy transport equation;

$$\frac{\partial \rho k}{\partial t} + \frac{\partial}{\partial x_j} \left(\rho u_j \frac{\partial k}{\partial x_j} - \left(\mu + \frac{\mu_\tau}{\sigma_k} \right) \frac{\partial k}{\partial x_j} \right) = \tau_{ij} S_{ij} - \rho \varepsilon + \phi_k \quad (6)$$

Energy dissipation transport equation;

$$\frac{\partial \rho \varepsilon}{\partial t} + \frac{\partial}{\partial x_j} \left(\rho u_j \varepsilon - \left(\mu + \frac{\mu_\tau}{\sigma_\varepsilon} \right) \frac{\partial \varepsilon}{\partial x_j} \right) = c_{\varepsilon 1} \frac{\varepsilon}{k} \tau_{ij} S_{ij} - c_{\varepsilon 2} f_2 \rho \frac{\varepsilon^2}{k} + \phi_\varepsilon \quad (7)$$

The SIMPLE (Semi-Implicit Method for Pressure Implicit Method for Pressure-Linked Equations) method was chosen as the solution method because of its robustness (Ansys Inc., 2022) and the quadratic solution was preferred.

Results and Discussion

Flow and temperature analyses of the drying kiln, which was designed to dry lumber, were simulated with the help of Ansys Fluent, and temperature and streamline contours are shown for a better understanding of the case. Figure 4 depicts the three-

dimensional streamlines contour of the drying kiln with 8 x 13 x 4 m dimensions, with 8 air inlets and 10 air outlet chimneys. In the given isometric representation, it is seen that the flow is divided into two main bodies. After the air comes from the fans and hits the concrete floor, it is divided into two in +z and -z directions, and it is observed that vortices are formed. While the flow velocity coming out of the fans is 5 m/s, the maximum flow velocity reached occurs near the chimneys and reaches approximately 10 m/s. As moved toward the middle of the vortices, the air velocity decreases and even approaches zero.

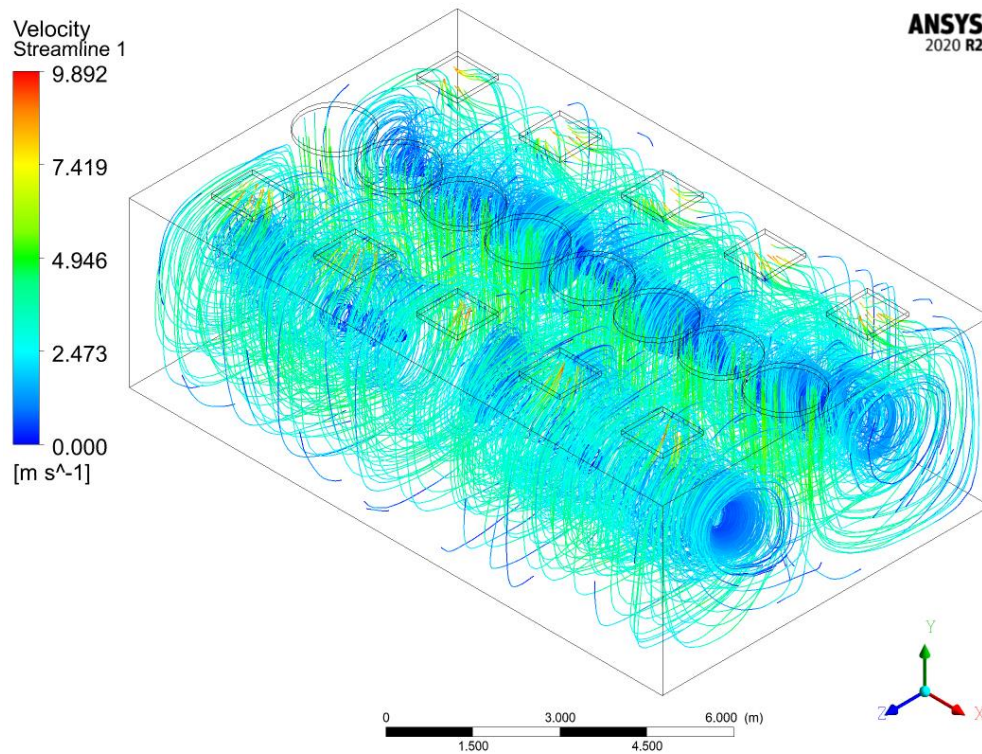


Figure 4. Three-dimensional streamline view of the kiln design

The mentioned separation in the flow can be seen more clearly in Figures 5 and 6. Streamlines are projected through the planes created at 2-meter intervals starting from the surface of the kiln in the -x direction. While the velocity approaches the maximum outside

the vortices, the velocity decreases when the streamlines are followed towards the center. The effect of the sharp-edged structure of the drying kiln on the flow can also be observed from the gaps formed.

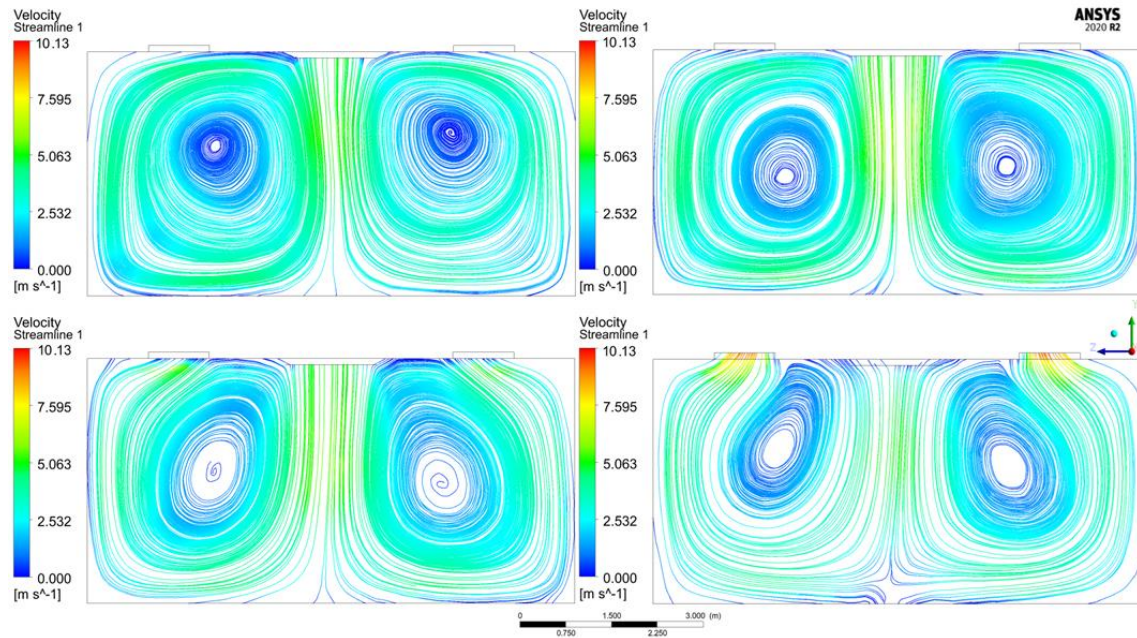


Figure 5. Streamlines view in the y-z plane (0-6 m)

The similarities draw attention to seven different intervals from which the streamlines are taken. Especially in the streamlines display at 6 meters, it is seen that the suction

is effective on the discharge side and thus the speed reaches the highest levels. This phenomenon can also be seen when color tones change from green to red tones.

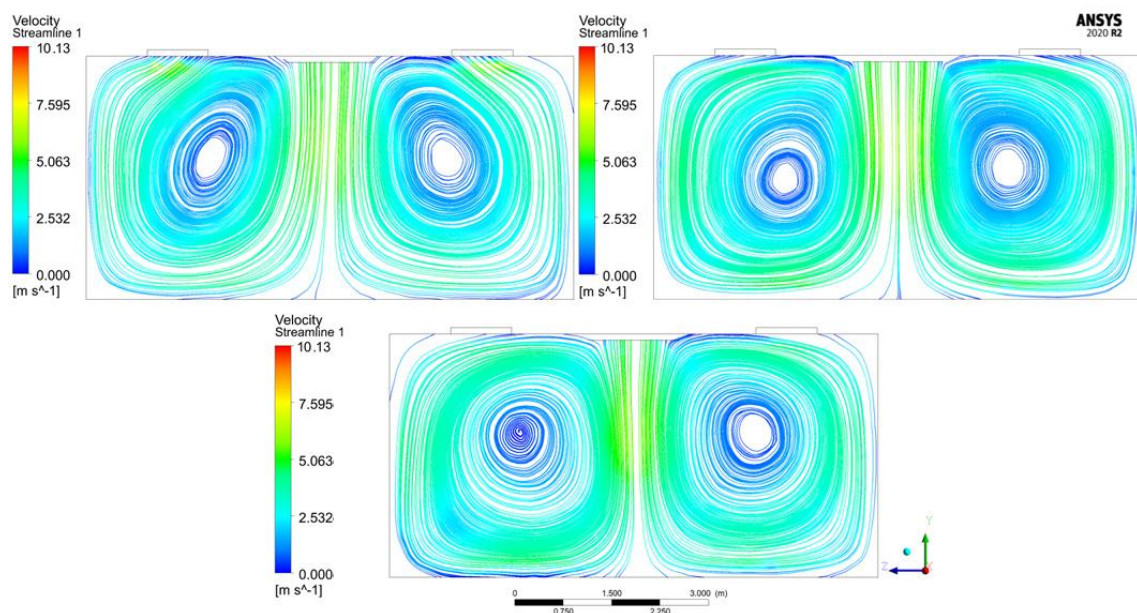


Figure 6. Streamlines view in the y-z plane (8-12 m)

Temperature contours of the lumber-drying kiln design Figures 7 and 8. When the temperature contours are examined, a

homogeneous temperature distribution is observed, regardless of the parts, except for the first and last contours.

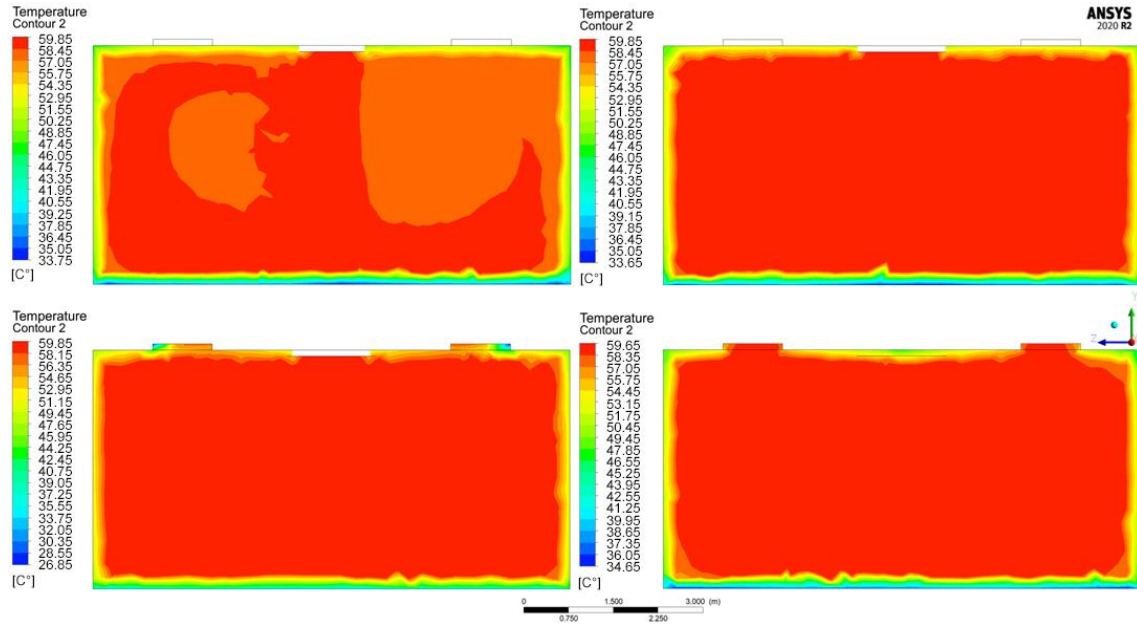


Figure 7. Temperature contours in the y-z plane (0-6 m)

The lowest temperature in the contours is 26.85°C (300K), the wall temperature entered in the simulation and the highest temperature is the air inlet temperature of 59.85°C (333K). In places close to the walls, the boundary layer

can be clearly distinguished from the contour color change. Heat transfer occurs between the walls and the drying air, and the walls are trying to be heated by the hot air.

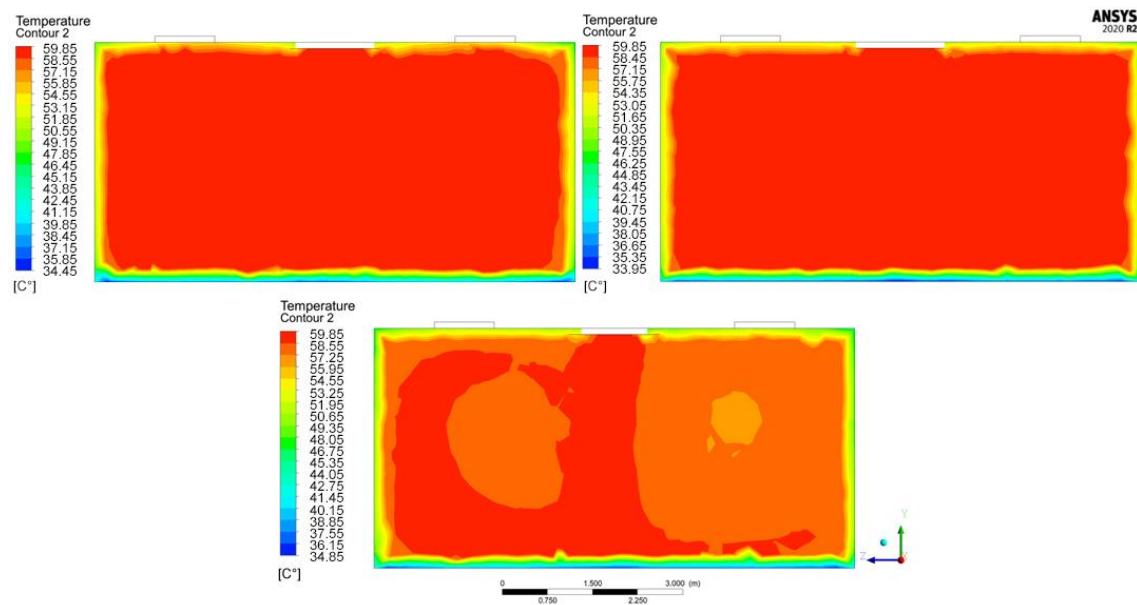


Figure 8. Temperature contours in the y-z plane (8-12 m)

It is thought that the difference in the first and seventh temperature contours is due to this reason, that is, the temperature decreases slightly in the parts close to the wall. It is also observed that the floor is determined as concrete and therefore the heat transfer is slower than aluminum panels. A kiln with fans parallel to the ground generates one big streamline that travels the kiln boundaries from wall-ground-wall-ceiling. However, as can be seen in the results, when locating the fans perpendicular to the ground, two effective streamlines were generated.

Differences between the two configurations will be figured out by an ongoing experimental study both for hardwood and softwood species. It is thought that the difference in the first and seventh temperature contours is due to this reason, that is, the temperature decreases slightly in the parts close to the wall. It is also observed that the floor is determined as concrete and therefore the heat transfer is slower than aluminum panels.

A kiln with fans parallel to the ground generates one big streamline that travels the kiln boundaries from wall-ground-wall-ceiling. However, as can be seen in the results, when locating the fans perpendicular to the ground, two effective streamlines were generated. Differences between the two configurations will be figured out by an ongoing experimental study both for hardwood and softwood species.

In the nature of things, surfaces interact with their surroundings. Therefore, the outer layers of things are affected more than the inner or core layers. Moreover, if the thing has complex pass-ways to the interior, the influence of surrounding factors causes variation between the layers. When the complex nature of wood has been taken into consideration, these variations become more crucial while the drying process. Due to this significant issue, industrial drying of wood requires advanced tools to figure out these variations and obtain proper drying. In this study, just CFD and thermal analysis of unloaded lumber-drying kiln was evaluated and these factors were not taken into consideration but the following project aims to figure out these issues.

Balancing its MC to its surrounding is the characteristic feature of wood. While doing that, dimensional changes in three essential axes (longitudinal, radial, and tangential) occur and dimensional instability is one of the challenging areas of wood science and technology because as Üçüncü et al. (2017) expressed formation of cracking, crooking, twisting, etc. faults while drying adversely influence the wood utilization. Therefore, the moisture range of the site where wood or wood-based products are used should be known and wood components of any product should be dried considering the target surrounding conditions.

Conclusion

First of all, the empty state of the drying kiln was analyzed, as so where and how often the lumbers were to be placed and dried. Considering the streamlines and temperature contours taken, it is seen that positioning should be done by leaving the vortex centers empty as much as possible or by directing the flow in a different way. It is aimed to put wooden piles in the parts left empty due to the vortex, and thus it is desired that the flow creates a homogeneous flow around the pile as much as possible. The formation of two different vortex paths may mean placing the timber to be dried in two lines. It is seen that placing the timbers in line with the chimney outlets can be advantageous in terms of drying speed and time. Proper thermal insulation of the floor and walls will also be beneficial for timber placed close to the floor and wall. Another way to overcome this is to leave these parts blank or by placing a material that will not be dried. In this way, the best lumber layout can be predicted, which can provide an advantage in terms of optimization of the kiln design to be loaded and dried.

Ethics Committee Approval

N/A

Peer-review

Externally peer-reviewed.

Author Contributions

Conceptualization: M.A.; Investigation: M.A., Y.F.G.; Material and Methodology: Y.F.G.; Supervision: M.A., Y.F.G.;

Visualization: M.A., Y.F.G.; Writing-Original Draft: M.A., Y.F.G.; Writing-review & Editing: M.A., Y.F.G.; Other: All authors have read and agreed to the published version of manuscript

Conflict of Interest

The authors declare that they have no conflict of interest.

Funding

N/A

References

- Ansys Inc. (2011). *Introduction to Ansys Meshing* (pp. L5-16). Ansys Inc.
- Ansys Inc. (2015). Mesh Quality And Advanced Topics Ansys Workbench 16.0. In *Ansys*.
- Ansys Inc. (2022). *Ansys Fluent 12.0 User's Guide*.
- Aydın, I. & Colakoglu, G. (2008). Variations in Bending Strength and Modulus of Elasticity of Spruce and Alder Plywood after Steaming and High Temperature Drying. *Mechanics of Advanced Materials and Structures*, 15(5), 371-374.
<https://doi.org/10.1080/15376490801977692>
- Bardina, J.E., Huang, P.G. & Coakley, T.J. (1997). Turbulence Modeling Validation. In *28th Fluid Dynamics Conference* (Issue April).
<https://doi.org/10.2514/6.1997-2121>
- Bernard, P.S. & Wallace, J.M. (2002). *Turbulent Flow: Analysis, Measurement and Prediction*. John Wiley & Sons, Inc.
- Bian, Z. (2001). Airflow and Wood Drying Models for Woodkilns. In *University of Science & Technology*.
- Budakçi, M., Aydın, M., Aşkun, T. & Güner, P. (2018). Antimicrobial Properties of Wood Water Obtained by a High-Frequency Vacuum Drying Method. *The Online Journal of Science and Technology*, 8(3), 21-25.
- Ciritcioğlu, H.H., Tarmian, A., Görgün, H.V. & Ünsal, Ö. (2022). Using Acoustic Emission Technique for Detecting Checks on Industrial-Size Beech Wood Disks During Drying. *Drying Technology*, 40(16), 3614-3621.
<https://doi.org/10.1080/07373937.2022.2073366>
- Duláu, M. & Madaras, I. (2019). Development of a Monitoring and Control System for Timber's Drying Process. *Procedia Manufacturing*, 32, 545-552.
<https://doi.org/10.1016/j.promfg.2019.02.251>
- Elustondo, D.M. & Oliveira, L. (2009). Model to Assess Energy Consumption in Industrial Lumber Kilns. *Maderas: Ciencia y Tecnologia*, 11(1), 33-46.
- Erriguible, A., Bernada, P., Couture, F. & Roques, M. A. (2005). Modeling of Heat and Mass Transfer at the Boundary Between a Porous Medium and its Surroundings. *Drying Technology*, 23(3), 455-472.
<https://doi.org/10.1081/DRT-200054119>
- Erriguible, A., Bernada, P., Couture, F. & Roques, M. (2006). Simulation of Superheated Steam Drying from Coupling Models. *Drying Technology*, 24(8), 941-951.
<https://doi.org/10.1080/07373930600776019>
- Fletcher, C.A.J. (1998). *Computational Techniques for Fluid Dynamics 1. In Computational Techniques for Fluid Dynamics 1*.
<https://doi.org/10.1007/978-3-642-58229-5>
- Ghiaus, A.G., Filios, A.E., Margaritis, D.P. & Tzempelikos, D.A. (2010). Industrial Drying of Wooden Pallets-CFD Analysis of Air Flow. *17th International Drying Symposium, 3-6 October, Germany*.
- Görgülü, Y.F., Özgür, M.A. & Köse, R. (2021). CFD Analysis of a NACA 0009 Aerofoil at a Low Reynolds Number. *Politeknik Dergisi*, 24(3), 1237-1242.
<https://doi.org/10.2339/politeknik.877391>
- Görgün, H.V. & Ünsal, Ö. (2020). Continuous Lumber Drying Kilns. *Bartın Orman Fakültesi Dergisi*, 22(1), 283-293.
- Guler, C. & Dilek, B. (2020). Investigation of High-Frequency Vacuum Drying on Physical and Mechanical Properties of Common Oak (*Quercus robur*) and Common Walnut (*Juglans regia*) Lumber. *BioResources*, 15(4), 7861-7871.
<https://doi.org/10.15376/biores.15.4.7861-7871>
- Hızıroğlu, S. (2017). *Fundamental Aspects of Kiln Drying Lumber*. Oklahoma Cooperative Extension Service.
- Hughes, B.R., & Oates, M. (2011). Performance Investigation of a Passive Solar-Assisted Kiln in the United Kingdom. *Solar Energy*, 85(7), 1488-1498.
<https://doi.org/10.1016/j.solener.2011.04.003>
- Hui-hui, S., Ping, Y., Le-yang, F. & Xin-yue, Z. (2015). Numerical Simulation of Hot Air Drying Kiln Velocity Field Based on Computational Fluid Dynamics. *International Journal of Research in Engineering and Science (IJRES)*, 3(5), 9-13.
- Jamaledine, T.J., & Ray, M.B. (2010). Application of Computational Fluid Dynamics for Simulation of Drying Processes: A Review. *Drying Technology*, 28(2), 120-154.
<https://doi.org/10.1080/07373930903517458>
- Janjai, S., Intawee, P. & Kaewkiew, J. (2010). A Solar Timber Drying System: Experimental Performance and System Modeling.

- International Energy Journal*, 11(3), 131–144.
- Jones, W.P. & Launder, B.E. (1972). The Prediction of Laminarization with a Two-equation Model of Turbulence. *Int. J. Heat Mass Transfer*, 15(2), 301-314. [https://doi.org/10.1016/0017-9310\(72\)90076-2](https://doi.org/10.1016/0017-9310(72)90076-2)
- Korkmaz, H., Ünsal, Ö., Görgün, H.V. & Avcı, E. (2020). Kereste Kurutmada Enerji Verimliliği-Güneş Enerjisi İle Kızılçam (*Pinus brutia*) Kerestesi Kurutma Örneği. *Politeknik Dergisi*, 23(3), 671-676. <https://doi.org/10.2339/politeknik.528103>
- Korkut, S., As, N. & Büyüksarı, Ü. (2018). Comparison of Two Kiln-Drying Schedules for Turkish Hazel (*corylus colurna*) Lumber of 5-Cm Thickness. *Maderas: Ciencia y Tecnologia*, 20(1), 129-138. <https://doi.org/10.4067/S0718-221X2018005011101>
- Kuriakose, R. & Anandharamkrishnan, C. (2010). Computational Fluid Dynamics (CFD) Applications in Spray Drying of Food Products. *Trends in Food Science and Technology*, 21(8), 383-398. <https://doi.org/10.1016/j.tifs.2010.04.009>
- Launder, B. E., & Sharma, B. I. (1974). Application of the Energy-Dissipation Model of Turbulence to the Calculation of Flow Near a Spinning Disc. *Letters in heat and mass transfer*, 1(2), 131-137. [https://doi.org/10.1016/0094-4548\(74\)90150-7](https://doi.org/10.1016/0094-4548(74)90150-7)
- Lee, C.J., Hwang, J.W. & Oh, S.W. (2022). Effect of Combined Radio-Frequency/Vacuum-Press Drying on the Strength Properties of Japanese larch Board. *Drying Technology*, 40(14), 2849-2856. <https://doi.org/10.1080/07373937.2021.1967972>
- Marshall, E.M. & Bakker, A. (2009). Computational Fluid Mixing. In *Food Mixing: Principles and Applications*. Fluent Inc. 257-345. <https://doi.org/10.1002/0471451452.ch5>
- Norton, T. & Sun, D.W. (2006). Computational Fluid Dynamics (CFD) - an Effective and Efficient Design and Analysis Tool for the Food Industry: A Review. *Trends in Food Science and Technology*, 17(11), 600-620. <https://doi.org/10.1016/j.tifs.2006.05.004>
- Norton, T., Sun, D.W., Grant, J., Fallon, R. & Dodd, V. (2007). Applications of Computational Fluid Dynamics (CFD) in the Modelling and Design of Ventilation Systems in the Agricultural Industry: A Review. *Bioresource Technology*, 98(12), 2386-2414. <https://doi.org/10.1016/j.biortech.2006.11.025>
- Özşahin, Ş., Demir, A. & Aydın, İ. (2019). Optimization of Veneer Drying Temperature for the Best Mechanical Properties of Plywood via Artificial Neural Network. *Journal of Anatolian Environmental and Animal Sciences*, 4(4), 589-597. <https://doi.org/10.35229/jaes.635302>
- Rumsey, C. (2021). *Turbulence Modeling Resource The Wilcox k-omega Turbulence Model*. Langley Research Center Turbulence Modeling Resource. <https://turbmodels.larc.nasa.gov/wilcox.html>
- Smit, G.J.F., du Plessis, J.P., & du Plessis, J.P. (2007). Modelling of Airflow Through a Stack in a Timber-Drying Kiln. *Applied Mathematical Modelling*, 31(2), 270-282. <https://doi.org/10.1016/j.apm.2005.11.003>
- Sun, D.W. (2007). Computational Fluid Dynamics in Food Processing. In *Computational Fluid Dynamics in Food Processing* (Second). Taylor & Francis. <https://doi.org/10.1201/b16696-16>
- Tarmian, A., Ciritcioğlu, H.H., Ünsal, Ö., Ahmadi, P., Gholampour, B., et al. (2022). Efficiency of Radiofrequency-Vacuum (RF/V) Technology for Mixed-Species Drying of Wood Disks with Inherent Defects. *Drying Technology*, 40(5), 1002-1012. <https://doi.org/10.1080/07373937.2020.1833214>
- Tuscarora Wood Midwest. (2021). *Why Kiln Dry Wood?* [Tuscarora Wood Midwest. <https://www.tuscarorawoodmidwest.com/tuscarora-news/why-kiln-dry-wood/>
- Üçüncü, K., Aydın, A. & Tiryaki, S. (2017). Experimental Investigation of Wood Moisture Change in Heated Indoor Climate Conditions. *İleri Teknoloji Bilimleri Dergisi*, 6(3),632-645.
- Ünsal, Ö., Dündar, T., Görgün, H.V., Kaymakci, A., Korkut, S., et al. (2020). Optimizing Lumber Drying Schedules for Oriental Beech and Sessile Oak Using Acoustic Emission. *BioResources*, 15(3), 6012-6022. <https://doi.org/10.15376/biores.15.3.6012-6022>.
- Vaz Jr, M., Zdanski, P.S.B., Cerqueira, R.F. & Possamai, D.G. (2013). Conjugated Heat and Mass Transfer in Convective Drying in Compact Wood Kilns: A System Approach. *Advances in Mechanical Engineering*, 5, 538931. <https://doi.org/10.1155/2013/538931>
- Versteeg, H.K. & Malalasekera, W. (2007). *An Introduction to Computational Fluid Dynamics*. In *Actas Urologicas Espanolas* (Second Edi, Issue 5). Pearson.
- Ward, J.C. (1991). Drying Defects. In W.T. Simpson (Ed.), *Dry kiln operator's manual* (179-205). USDA Forest Product Laboratory.

<https://doi.org/10.1016/b978-0-08-010635-9.50011-2>

Wilcox, D.C. (2006). *Turbulence Modeling for CFD*. DCW Industries.

Xia, B. & Sun, D.W. (2002). Applications of Computational Fluid Dynamics (CFD) in the Food Industry: A Review. *Computers and Electronics in Agriculture*, 34(1-3), 5-24.
[https://doi.org/10.1016/S0168-1699\(01\)00177-6](https://doi.org/10.1016/S0168-1699(01)00177-6)